$Pb[Cu(SO_4)(OH)_2]$: A Quasi-One-Dimensional $S = 1/2$ Magnet with Ferromagnetic Nearest-Neighbor and Antiferromagnetic Next-Nearest-Neighbor Exchange Interactions

R. Szymczak, H. Szymczak
Institute of Physics, Polish Academy of Sciences, al. Lotników 32/46, 02-668 Warsaw, Poland
G. Kamieniarz, G. Szukowski, K. Jaśniewicz-Pacer, W. Florek
Faculty of Physics, A. Mickiewicz University, Umultowska 85, 61-614 Poznań, Poland
V. Maltsev
Department of Geology, Moscow State University, 119899 Moscow, Russia
and G.-J. Babonas
Semiconductor Physics Institute, 2600 Vilnius, Lithuania

(Received October 28, 2008; in final form March 25, 2009)

Magnetic properties of $Pb[Cu(SO_4)(OH)_2]$ (linarite) natural single crystals were studied by magnetization and specific heat measurements. The angular dependences of magnetization were revealed which correlated with the regularities of the crystal structure. At about 2.8 K this quasi-one-dimensional Heisenberg system undergoes a phase transition to the long-range antiferromagnetic order with antiparallel magnetic moments aligned probably along the ***b***-axis. The antiferromagnetic order is evidenced by the metamagnetic transition and pronounced λ-type anomaly at T_N in the specific heat. Using phenomenological modeling based on a quantum transfer-matrix method, we argue that at higher temperatures linarite is a quasi-one-dimensional system with competing ferromagnetic nearest-neighbor and antiferromagnetic next-nearest-neighbor exchange interactions.

PACS numbers: 75.40.Cx, 75.50.Ee, 75.30.Gw, 75.30.Et, 75.30.Kz

1. Introduction

Recently, quantum effects in one-dimensional spin systems have attracted widespread and general interest. The properties of such systems are strongly affected by quantum fluctuations. In spite of their simplicity, the one-dimensional spin systems involve rich physics. For the $S = 1/2$ antiferromagnetic Heisenberg chain, the theory predicts a highly nontrivial ground state, which is the quantum liquid state with no classical counterpart.

Many of the one-dimensional (1D) antiferromagnets have the energy gap due to frustrated spin interactions. Analytical and numerical studies [1–3] of a frustrated Heisenberg chain model have shown a transition from a gapless phase for $\alpha < \alpha_{\rm crit}$ to a gapped phase for $\alpha > \alpha_{\rm crit}$, where $\alpha = J_2/J_1$, and J_1, J_2 denote the nearest-neighbor (nn) and the next nearest-neighbor (nnn) antiferromagnatic interactions, respectively. The value of $\alpha_{\rm crit}$ was estimated by numerical methods to be 0.241 [4]. In the gapped phase the ground state is the singlet ($S = 0$) separated by the spin-gap from the excited triplet level ($S = 1$).

Recently, quite a new phenomenon has been discovered (see Ref. [5] for details and references), namely the impurity-induced antiferromagnetic phase in one-dimensional spin-gap systems. This phenomenon was observed for the first time in doped spin-Peierls compound $CuGeO_3$ [5]. The possibility of such long-range magnetic order was shown theoretically [6, 7] for the spin-Peierls system. Very recently a transition to an ordered magnetic Néel state was observed in an undoped (pure) organic spin-Peierls system p-CyDOV [8]. Motivated by this observation a theoretical model was developed which manifests the onset of a Néel ordering in a spin-Peierls state for nonzero temperatures [9].

Much of the work on the frustrated system has been focused on the case when both nn and nnn interactions are antiferromagnetic. But the frustrated regime is also predicted for the case with ferromagnetic nn and antiferromagnetic nnn exchange interactions [10, 11]. Quite recently magnetic properties of $Rb_2Cu_2Mo_3O_{12}$ powder have been measured [12]. This compound was shown to be a one-dimensional spin 1/2 Heisenberg system with ferromagnetic first-nearest neighbor and antiferromagnetic second-nearest-neighbor competing interactions. A list of other similar compounds is provided in Ref. [12] and this list is still growing.

In this paper the properties of the linarite single crystal ($Pb[Cu(SO_4)\ (OH)_2]$) are studied by magnetization and specific heat measurements. Referring to the phenomenological modeling based on the quantum-transfer matrix (QTM) method, we argue that linarite belongs to the family of one-dimensional compounds with the competing ferromagnetic nn and antiferromagnetic nnn exchange interactions.

Linarite ($Pb[Cu(SO_4)(OH)_2]$) crystal has the space group symmetry $P2_1/m$ and the lattice parameters $a = 9.701(2)$ Å, $b = 5.650(2)$ Å, $c = 4.690(2)$ Å, $\beta = 102.65(2)^\circ$ [13, 14]. Cu^{2+} ions ($S = 1/2$) located in Cu–O chains determine the magnetic properties of linarite. Each of these Cu ions (Fig. 1) is fourfold coordinated. The surrounding oxygen atoms O(4) and O(5) (the notation O(i) is introduced to distinguish different oxygen positions; $i = 1$–5), form a flat tetragon close to the square. The distances from Cu to O(4) and O(5) are equal to 1.927 Å, and 1.976 Å, respectively. The O(4) and O(5) atoms in the CuO_4 squares belong to the hydroxyl (OH) groups. The coordination figure is completed by two further oxygen atoms O(3), yielding a distorted octahedron with Cu–O(3) distances of about 2.539 Å.

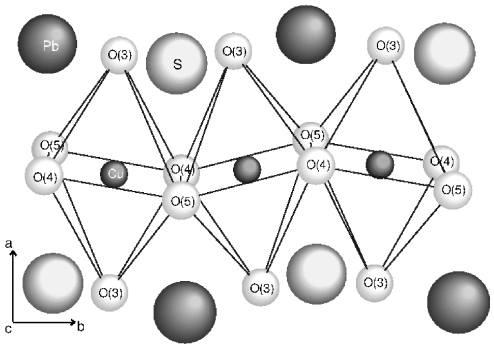

Fig. 1. A sketch of the Cu–O ribbon together with its neighborhood.

The CuO_4 plaquettes compose roof-shaped, staggered, Cu–O ribbons along the ***b***-axis and the dihedral angle between each two neighboring planes amounts to about 155°. The oxygen atoms O(3) apical to CuO_4 squares together with O(1) and O(2) atoms compose the tetrahedral surrounding of S^{6+} ion of $(SO_4)^{2-}$ radical. The $(SO_4)^{2-}$ tetrahedra as well as Pb atoms decorate alternatively both sides of the Cu–O ribbon. It shows that in linarite, similarly as in $CuGeO_3$, the structural unit characteristic of cuprates [15] is the Cu–O ribbon composed of the sharing edges CuO_4 squares.

The results of the zero-field susceptibility measurements were reported in detail earlier [16] and were fitted within the model with both the nn and nnn couplings.

2. Experiment

2.1. Structural features of linarite

The samples investigated were natural crystals of linarite mineral. Neither chemical nor thermal treatment was used. According to the data of the X-ray diffraction they could be treated as single crystals. The composition of the sample was tested by electron probe microanalysis (EPMA) using a commercial EPMA apparatus (LINK-Isis of Oxford Instruments) together with an electron microscope (JEOL 35). The chemical composition of studied samples, determined from the analysis in 15 points corresponding to linarite, was the following: $(Pb_{0.95}Sr_{0.05})[Cu_{1-x}(SO_{4-y})(O_{1-z}H)_2]$, where the mean deficit of copper $x \approx 7\%$ and the total mean deficit of oxygen $(y + z) \approx 13\%$. There were found some small inclusions corresponding to nonstoichiometric anglesite ($PbSO_4$) in amount less than 5% of crystal volume.

We note that the deficit of copper and oxygen may lead to the chemical disorder having impact on magnetic properties similar to those observed in $CuGeO_3$ doped with Zn (a disorder on the spin sites) and Si (a disorder on the side chains). However, in our subsequent analysis we neglect the presence of defects in the sample.

2.2. Measurements and results

The magnetic properties of linarite were studied with a commercial SQUID magnetometer (Quantum Design, MPMS-5) in the temperature range 2–300 K and in magnetic fields up to 50 kOe. The temperature dependence of magnetic susceptibility, $\chi(T) = M(T)/H$, was measured in various magnetic fields applied both along the symmetry 2_1 axis (***b***-axis), i.e. along the Cu–O chains, as well as along the ***a*** and ***c*** axes.

As an example, the $\chi(T)$ dependence measured in $H = 6$ kOe ($H \| \boldsymbol{b}$) is presented in Fig. 2. It is remarkable that the magnetic susceptibility decreases rapidly below 4 K. At $T < 3$ K an anomaly was found in the $\chi(T)$ dependence for all the directions. This anomaly is clearly seen in $\mathrm{d}\chi/\mathrm{d}T$ (Fig. 3) for the field in the ***b*** direction. The pronounced peak at $T_N \approx 2.7$ K indicates the onset of a long-range antiferromagnetic (AF) ordering for $T < T_N$. The non-linearity in $M(H)$ dependences measured below T_N in magnetic field applied along the ***b***-axis gives the evidence of AF order (see inset in Fig. 3). Moreover, the appearance of this metamagnetic transition at low temperatures implies that magnetic moments in AF phase are presumably directed along the ***b***-axis.

In order to estimate the magnetization anisotropy, we measured the magnetic moment of the sample versus magnetic field direction. The sample rotation axis was always perpendicular to the magnetic field direction. The orientation-dependent magnetic moment measured at $T = 5$ K in $H = 6$ kOe is presented in Fig. 4. The measurements were done in two configurations (for two rotation axes — both lying in the natural crystallographic $(\bar{1}01)$ plane):

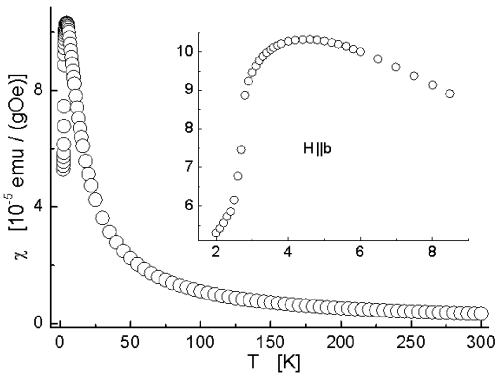

Fig. 2. Example of experimental data of the magnetic susceptibility $\chi = M/H$ measured in $H = 6$ kOe directed along the $\boldsymbol{b}$-axis, as a function of temperature (in the inset the same values are presented in the enlarged scale in a low temperature region).

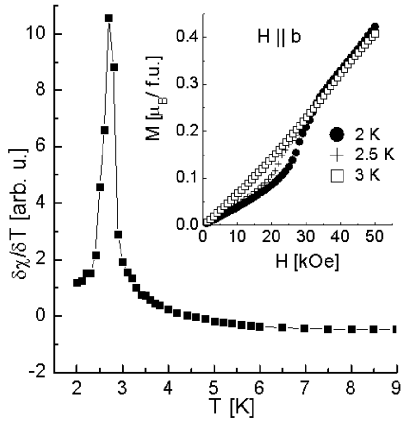

Fig. 3. The temperature derivative of the magnetic susceptibility versus temperature. The inset shows the low temperature magnetization vs. magnetic field. The continous line is guide to the eyes.

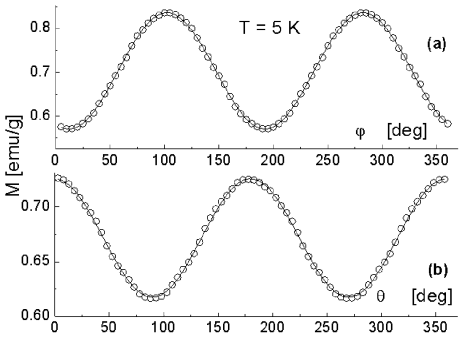

Fig. 4. Angular dependences of magnetization measured in $H = 6$ kOe at $T = 5$ K. (a) Magnetic field in the (ac) plane; φ is the angle between the magnetic field direction and the $\boldsymbol{a}$-axis. (b) Magnetic field in the plane containing the $\boldsymbol{b}$-axis and the normal to the ($\bar{1}01$) plane; θ — the angle between the magnetic field direction and the normal to the ($\bar{1}01$) plane. The continous lines are guide to the eyes.

(i) the sample was rotated around the $\boldsymbol{b}$-axis (this case corresponds to the rotation of magnetic field in the ($\boldsymbol{ac}$) plane). The maximum of magnetization ($M_{\max 1} \approx 0.84$ emu/g) was obtained at $\boldsymbol{H} \| \boldsymbol{c}$-axis (see Fig. 4a). The minimum of magnetization ($M_{\min 1} \approx 0.57$ emu/g) was obtained at $\boldsymbol{H} \perp \boldsymbol{c}$-axis;

(ii) the sample was rotated around the direction perpendicular to the $\boldsymbol{b}$-axis (this case corresponds to the rotation of magnetic field in the plane containing the $\boldsymbol{b}$-axis and the normal to the ($\bar{1}01$) plane). Below, the latter direction will be denoted as $\boldsymbol{n}$ and consequently the rotation in the ($\boldsymbol{bn}$) plane is used for this case. The maximum of magnetization ($M_{\max 2} \approx 0.73$ emu/g) was obtained at $\boldsymbol{H} \| \boldsymbol{n}$ (i.e. $\boldsymbol{H} \perp \boldsymbol{b}$-axis, see Fig. 4b), whereas the minimum of magnetization ($M_{\min 2} \approx 0.62$ emu/g) was obtained at $\boldsymbol{H} \| \boldsymbol{b}$-axis.

The anisotropy of magnetization (see Figs. 4, 5) can be described, determining the components of susceptibility tensor χ_{ij}. Taking into account the symmetry of the crystal, this tensor has five nonzero components χ_{xx}, χ_{yy}, χ_{zz}, $\chi_{xz=zx}$ in the orthogonal $\boldsymbol{xyz}$ coordinate system with $\boldsymbol{x} \| \boldsymbol{a}$-axis and $\boldsymbol{y} \| \boldsymbol{b}$-axis. The angle between $\boldsymbol{z}$-axis and the $\boldsymbol{c}$-axis is equal to 12.65°.

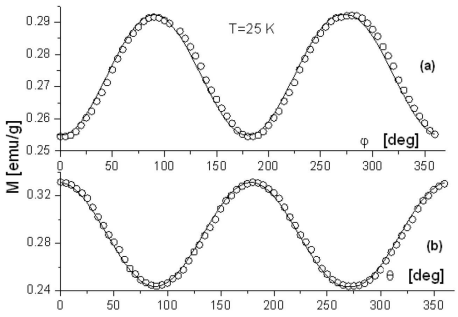

Fig. 5. Angular dependences of magnetization measured in $H = 6$ kOe at $T = 25$ K. (a) Magnetic field in the (ac) plane; φ is the angle between the magnetic field direction and the $\boldsymbol{a}$-axis. (b) Magnetic field in the plane containing the $\boldsymbol{b}$-axis and the normal to the ($\bar{1}01$) plane; θ — the angle between the magnetic field direction and the normal to the ($\bar{1}01$) plane. The continous lines are guide to the eyes.

The magnetization measured in configuration (i) (magnetic field in the ($\boldsymbol{ac}$) plane) can be described in terms of the symmetric χ_{ij} tensor components in the following way:

$$M_{ac} = H(\chi_{xx} \cos^2 \varphi + \chi_{xz} \sin 2\varphi + \chi_{zz} \sin^2 \varphi), \quad (1)$$

where φ is an angle between magnetic field direction and the $\boldsymbol{a}$-axis, and M_{ac} is a magnetization measured along the magnetic field direction.

For the configuration (ii) the magnetization in the ($\boldsymbol{bn}$) plane along the field direction can be described as follows:

$$M_{bn} = H[(\chi_{xx} \cos^2 \varphi_0 + \chi_{xz} \sin 2\varphi_0 + \chi_{zz} \sin^2 \varphi_0) \cos^2 \theta + \chi_{yy} \sin^2 \theta]. \quad (2)$$

Here, θ is the angle between the magnetic field direc-

tion and the normal to the $(\bar{1}01)$ plane, $\boldsymbol{n}$, and $\varphi_0 \approx 62^\circ$ is the angle between the $\boldsymbol{a}$-axis and the $\boldsymbol{n}$ direction.

The best fit of relations given in Eq. (1) and Eq. (2) to the experimental data for $T = 5$ K and $T = 25$ K, represented by the solid lines in Fig. 4 and Fig. 5, respectively, yielded the following χ_{ij} tensor components (values in [emu/mole Oe]):

$$\chi^{(1)} = \begin{pmatrix} 0.039 & 0 & -0.004 \\ 0 & 0.041 & 0 \\ -0.004 & 0 & 0.055 \end{pmatrix},$$

$$\chi^{(2)} = \begin{pmatrix} 0.016 & 0 & -0.001 \\ 0 & 0.017 & 0 \\ -0.001 & 0 & 0.022 \end{pmatrix}.$$

The corresponding tensor components χ'_{ij} in the system of principal axes are (0.038, 0.041, 0.056) for $\chi^{(1)}$ and those of $\chi^{(2)}$ amount approximately to its diagonal elements. These values indicate that in the principal axes system $g'_{xx} \leq g'_{yy} < g'_{zz}$ which agrees qualitatively with the estimates of g-factors found earlier [16].

The above given susceptibility results suggest that anisotropy of magnetization within the limits of experimental errors is weak and weakly dependent on temperature. It means that components of g_{ij} tensor are also practically temperature independent because of a small value of orbital contributions to the g_{ij} tensor components. Following the method proposed by Metzger et al. [17], we have estimated the dipolar contribution to anisotropy energy that suggests that pure dipole–dipole magnetic interactions prevail in linarite and are stronger than anisotropic exchange interactions. It was also checked for various directions of magnetic field that the possible contribution to anisotropy due to the changes of demagnetization factors are negligible.

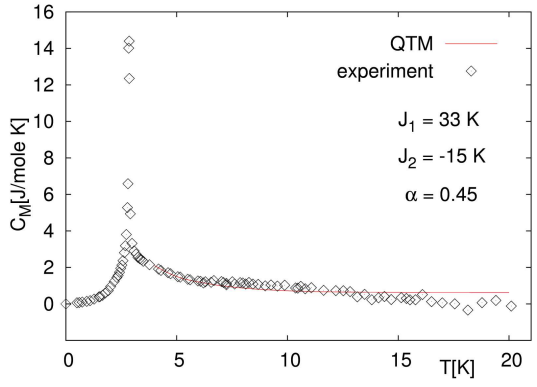

Fig. 6. The magnetic specific heat vs. temperature in zero magnetic field. The experimental data are plotted by the diamond symbols. The continous line presents the theoretical QTM temperature dependence for the parameters defined in the legend.

Heat capacity measurements were carried out $t < 20$ K using the adiabatic heat pulse method. At $T \approx 2.83$–2.86 K a sharp anomaly of the λ-like shape was found and attributed to the phase transition to the long-range AF order with the Néel temperature $T_{\rm N} \approx 2.84$ K. The specific heat C, falls down very rapidly just below $T_{\rm N}$ but it is distinctly enhanced for $T > T_{\rm N}$. The latter observation suggests a possible contribution (up to 15 K) from the short-range magnetic ordering in the low--dimensionalsystem. Far from the transition point, the lattice contribution estimated by the expression $C_{\rm L} = \beta T^3 + \gamma T^5$ dominates in the $C(T)$ dependence, where $\beta = 3.4 \times 10^{-3}$ J mol^{-1} K^{-4} and $\gamma = -3.8 \times 10^{-6}$ J mol^{-1} K^{-6}. From the coefficient β a Debye temperature of about 185 K was determined. The estimated magnetic contribution $C_{\rm M}(T) = C(T) - C_L(T)$ is displayed by the diamond symbols in Fig. 6.

3. Phenomenological modeling

Neglecting anisotropy and antisymmetric Dzyaloshinsky–Moriya interactions, the properties of the 1D spin-1/2 chains with the nn and nnn couplings and the bond alternation can be modeled by the Heisenberg Hamiltonian

$$\hat{H} = J_1 \sum_i \{[1 + (-1)^{-i}\delta]\hat{S}_i\hat{S}_{i+1} + \alpha\hat{S}_i\hat{S}_{i+2}\}, \qquad (3)$$

where $\hat{S}_i$ is the spin-1/2 operator, δ is the parameter describing bond alternation and $\alpha = J_2/J_1$ is the ratio of the nnn and nn coupling, related to frustration. The values $\alpha = 0$ and $\delta = 1$ correspond to the dimer limit of isolated spin pairs, whereas the uniform chain is described for $\alpha = 0$ and $\delta = 0$. For the alternating chain ($\alpha = 0$, $\delta \neq 0$) one normally regards the parameter δ to be independent of temperature.

At first the modeling with $\alpha = 0$ was attempted for the zero-field susceptibility $\chi(T)$. The numerical calculations of thermodynamic properties of the 1D system reported by Bonner and Fischer [18] for $\delta = 0$ and those by Hall et al. [19] for $\delta \neq 0$ were referred to. The fitting performed for our experimental data has indicated that the Bonner–Fischer ($\alpha = 0$, $\delta = 0$) and isolated dimers ($\alpha = 0$, $\delta = 1$) models deviate distinctly from the experiment. The fitting procedure carried out in the framework of the alternating-chain model ($\alpha = 0$, $\delta \neq 0$, $\delta \neq 1$), based on the approximate formula given by Hall et al. [19] valid for $k_{\rm B}T/J_1 \geq 0.25$, led to the values $\delta = 0.1$ and $J_1 = 7$ K. This value of the bond alternation parameter is hard to accept, taking into account the X-ray diffraction data which show identical surrounding for each Cu ion (Fig. 1).

Having no analytical expression for $\chi(T)$ in the case $\alpha \neq 0$ and $\delta = 0$, the fitting procedure was based on the numerically exact QTM method applied earlier to $CuGeO_3$ results [20]. Analyzing only the experimental susceptibility data for three crystallographic directions [16], the following exchange couplings: $J_1 = -30 \pm 5$ K, $\alpha = -0.50 \pm 0.05$ and the following g factors: $g_a = 2.00$, $g_b = 2.19$, $g_c = 2.30$ were obtained. It

means that the nn interactions have ferromagnetic character while nnn interactions are antiferromagnetic. Since for the studied system the ratio $J_2/J_1 < -0.25$, this competing system has an incommensurate ground state with the total spin $S_{tot} = 0$ [10].

Having measured the magnetic specific heat data (Fig. 6), the numerical simulations of the specific heat for Hamiltonian (3) can be performed within the QTM technique. We have checked here that for $\delta = 0.1$, $J_1 = 7$ K and $\alpha = 0$, the specific heat curve appears to be consistent with experiment above 8 K but deviates significantly for lower temperatures. In order to reach an agreement with experiment, the coupling should be diminished down to 5 K, affecting the susceptibility fit. Assuming two antiferromagnetic couplings ($\alpha \neq 0$) and imposing $\delta = 0$, the susceptibility fitting results in the parameters $J_1 = 6.7$ K and $J_2 = 2.0$ K. Quality of the susceptibility fit is inferior to that found for $J_1 = -30 \pm 5$ K, $\alpha = -0.50 \pm 0.05$, however. Moreover, the specific heat curve looks similar to that for $\delta = 0.1$.

Finally, assuming the ferro- and antiferromagnetic interactions, the acceptable overall fit to the experimental specific heat could be obtained here for $J_1 = -33$ K, $\alpha = -0.45$ which are within the error bars of those found before ($J_1 = -30 \pm 5$ K, $\alpha = -0.50 \pm 0.05$) [16]. These data are plotted in Fig. 6 by the continous line. Agreement with experiment is particularly good in the low temperature region, where the experimental results are most reliable.

4. Discussion and conclusions

The fact that in this competing system with nonmagnetic ground state the 3D antiferromagnetic order appearing at low temperature is not unexpected. It was shown [21] that for $J_2/J_1 < -0.25$ the energy gap is strongly reduced to a very small value. It creates conditions favorable for appearance of antiferromagnetic order due to impurities [6, 7, 22, 23] reducing locally the spin gap. Another mechanism is also possible [24–27] when an impurity is assumed to cut the chains and generate randomly distributed localized free moments. These moments are weakly coupled by exchange interactions, caused by a virtual polarization of the singlet background. In the frames of this scenario the long range Néel order is developing, being stabilized by the interchain exchange. We expect that the first scenario is more likely for linarite, due to the Cu deficit and the system studied is almost pure one-dimensional with interchain interactions that can be neglected.

The nn superexchange determining the value of the exchange integral (J_1) can be realized through O(4) or O(5) oxygen atoms. The superexchange coupling between nn Cu atoms is realized with 94.3° and/or 91.3° bending of Cu–O–Cu bonds, through O(4) and O(5), respectively. The nature of Cu–O–Cu couplings in linarite could be expected to be ferromagnetic taking into account rather small deviation of the superexchange angle from 90°. According to Goodenough–Kanamori–Anderson (GKA) rule, the nn Cu–Cu coupling converts from AF to FM, as the bending of the Cu–O–Cu bond changes from 180° to 90°. These expectations well coincide also with results of Mizuno et al. [28] concerning properties of edge-sharing Cu–O chains, which determine also the magnetic properties of linarite. The sole member of cuprates with the same kind of Cu–O chains and with the superexchange relatively close to the orthogonality (99°) but with the AFM coupling of nn Cu atoms is $CuGeO_3$ [28]. However, this rather unexpected fact was explained by the proximity between Cu–O and Ge–O chains and by the influence of heavy side group (Ge) on the state of coupling oxygen (on its $2p$ orbitals) of Cu–O chain [29, 30]. Nevertheless, in linarite, with its the most probable FM superexchange path quite close to the orthogonality (91.3°), such effect should be much less important.

The nnn superexchange (J_2) along the ribbon may be realized through Cu–O(4)–O(5)–Cu. It is necessary to mention that the direct O(4)–O(5) bond may be assisted also by an additional hydrogen bond.

In conclusion, on the base of magnetic susceptibility [16], magnetization and specific heat measurements it was shown that linarite undergoes phase transition at about $T_N = 2.8$ K and below which the spin-flip transition occurs due to antiferromagnetic alignments of the magnetic moments ordering along the $\boldsymbol{b}$ axis. The system displays a weak anisotropy and sharp decrease in susceptibility below 4 K.

Theoretical analysis based on the phenomenological modeling and *ab initio* LSDA + U calculations leads to the in-chain coupling parameters J_1, J_2 that imply strong frustration due to the competing ferromagnetic nearest--neighbor and antiferromagnetic next-nearest-neighbor interactions ($\alpha < -0.25$) and the nonmagnetic ground state.

The unusual crystal structure and observed properties leading to the estimate $\alpha = -0.5$ make linarite a good candidate for a system displaying the quantum helimagnetism.

Acknowledgments

The authors are very grateful to Fersman Museum of Mineralogy, Russian Academy of Sciences (Moscow, Russia) for supplying the samples of linarite (No. 52863). The clarifying discussions with Drs. S. Drechsler, H. Rosner, V. Kataev and the technical assistance in experiments of Mrs. B. Krzymańska are greatly acknowledged. The high performance computing was carried out in PSNC Center in Poznań and on a local duster PEARL. The contribution of G.K. was partially supported by the grant No. N202 309835 of the Polish Ministry of Science and High Education and the Leibniz Institute IFW in Dresden. The support from the EU MAGMANet project No. NMP3-CT-2005-515767 is also acknowledged.

References

[1] K. Okamota, K. Nomura, *Phys. Lett. A* **169**, 433 (1992).

[2] R. Chitra, S. Pati, H.R. Krishnamurthy, D. Sen, S. Ramasesha, *Phys. Rev. B* **52**, 6581 (1995).

[3] A.A. Zvyagin, A. Klumper, *Phys. Rev. B* **68**, 144426 (2003).

[4] S. Eggert, *Phys. Rev. B* **54**, R9612 (1996).

[5] K. Uchinokura, *J. Phys., Condens. Matter* **14**, R195 (2002).

[6] H. Fukuyama, T. Tanimoto, M. Saito, *J. Phys. Soc. Jpn.* **65**, 1182 (1996).

[7] M. Mostovoy, D. Khomskii, J. Knoester, *Phys. Rev. B* **58**, 8190 (1998).

[8] K. Mukai, M. Yanagimoyo, S. Tanaka, M. Mito, T. Kawae, K. Takeda, *J. Phys. Soc. Jpn.* **72**, 2312 (2003).

[9] A.V. Zvyagin, A.V. Makarova, *J. Phys., Condens. Matter* **16**, 2673 (2004).

[10] T. Tonegawa, I. Harada, *J. Phys. Soc. Jpn.* **58**, 2902 (1989).

[11] R. Bursill, G.A. Gehring, D.J.J. Farnell, J.B. Parkinson, Tao Xiang, Chen Zeng, *J. Phys., Condens. Matter* **7**, 8605 (1995).

[12] M. Hase, H. Kuroe, K. Ozawa, O. Suzuki, H. Kitazawa, G. Kido, T. Sekine, *Phys. Rev. B* **70**, 104426 (2004).

[13] H. Effenberger, *Mineral. Petrol.* **36**, 3 (1987).

[14] R.K. Eby, F. Hawthorne, *Acta Crystallogr. B* **49**, 28 (1993).

[15] L. Leonyuk, V. Maltsev, G.-J. Babonas, R. Szymczak, H. Szymczak, M. Baran, *Acta Crystallogr. A* **57**, 34 (2001).

[16] G. Kamieniarz, M. Bieliński, G. Szukowski, R. Szymczak, S. Dyeyev, J.-P. Renard, *Comp. Phys. Commun.* **147**, 716 (2002).

[17] R.M. Metzger, N.E. Heimer, D. Gundel, H. Sixl, R.H. Harms, H.J. Keller, D. Nothe, D. Wehe, *J. Chem. Phys.* **77**, 6203 and 6210 (1982).

[18] J.C. Bonner, M.E. Fischer, *Phys. Rev. B* **135**, A640 (1964).

[19] J.W. Hall, W.E. Marsh, R.R. Weller, W.E. Hatfield, *Inorg. Chem.* **135**, 1033 (1981).

[20] G. Kamieniarz, M. Bieliński, J.-P. Renard, *Phys. Rev. B* **60**, 14 521 (1999).

[21] C. Itoi, S. Qin, *Phys. Rev. B* **63**, 224423 (2001).

[22] M. Saito, H. Fukuyama, *Physica B* **246-247**, 27 (1998).

[23] M. Saito, H. Fukuyama, *Physica B* **284-288**, 1565 (2000).

[24] G.B. Martins, E. Dagotto, J.A. Riera, *Phys. Rev. B* **54**, 16032 (1996).

[25] M. Fabrizio, R. Melin, J. Souletie, *Eur. Phys. J. B* **10**, 607 (1999).

[26] M. Mostovoy, D. Khomskii, *Z. Phys. B, Condens. Matter* **103**, 209 (1997).

[27] A. Dobry, P. Hansen, J. Riera, D. Augier, D. Poilblanc, *Phys. Rev. B* **60**, 4065 (1999).

[28] Y. Mizuno, T. Tohyama, S. Maekawa, T. Osafune, N. Motoyama, H. Eisaki, S. Uchida, *Phys. Rev. B* **57**, 5326 (1998).

[29] W. Geertsma, D. Khomskii, *Phys. Rev. B* **54**, 3011 (1996).

[30] D. Khomskii, W. Geertsma, M. Mostovoy, *J. Phys. (France)* **56**, 3239 (1997).